J Mater Sci (2015) 50:7488–7494
DOI 10.1007/s10853-015-9308-2

High-strength mullite fibers reinforced ZrO_2–SiO_2 aerogels fabricated by rapid gel method

Jian He[1] · Xiaolei Li[1] · Dong Su[1] · Huiming Ji[1] · Yingchen Qiao[1]

Received: 16 March 2015 / Accepted: 28 July 2015 / Published online: 1 August 2015

Abstract A rapid gelation process is adopted to fabricate mullite fibers-reinforced ZrO_2–SiO_2 (M/ZrO_2–SiO_2) aerogels. The short-cut mullite fibers are introduced into ZrO_2–SiO_2 sol via aging and supercritical drying, and the epoxides are used as gelation accelerators. The as-prepared M/ZrO_2–SiO_2 aerogels have a three-dimensional reticulated porous structure similar to those of pure ZrO_2–SiO_2 aerogels observed by scanning electron microscopy, which indicates that the addition of fibers does not obviously affect the morphology of aerogels. It is observed that the mullite fibers disperse in the aerogels homogeneously, and fibers combine well with aerogels. M/ZrO_2–SiO_2 aerogel composites exhibit high compressive strengths up to 0.438 MPa, which indicates that this structure benefits the loading transfer and thus enhances their mechanical properties. Moreover, the thermal conductivity of M/ZrO_2–SiO_2 aerogel composites is as low as that of the pure ZrO_2–SiO_2 aerogels ($\sim$0.0270 W m^{-1} K^{-1}).

✉ Xiaolei Li
lxlei@tju.edu.cn

✉ Dong Su
sudong@tju.edu.cn

Jian He
hejian@tju.edu.cn

Huiming Ji
jihuiming@tju.edu.cn

Yingchen Qiao
qyccailiao@163.com

[1] Key Lab of Advanced Ceramics and Machining Technology of Ministry of Education, School of Materials Science and Engineering of Tianjin University, Tianjin 300072, China

Introduction

Aerogels exhibit unique physical properties, chemical properties, and high-temperature resistance, which leads to its wide application in energy, chemical engineering, transportation electronic, and optical industries [1–5], such as Cerenkov detectors [6], thermal insulation [7], catalysis [8], storage media [9] etc. Among them, its application in thermal insulation is very important [10]. SiO_2 aerogel, a widely used aerogel, shows limited thermal stability with long time working temperature less than 650 °C, and poor high-temperature insulation because it is highly transparent in the special wavelength regions (i.e., from 3 to 8 μm) [11]. Additionally, it displays poor mechanical properties under compressive strength of less than 0.1 MPa at 10 % strain. Moreover, it is always very fragile [12, 13]. As a result, these drawbacks hinder the application of SiO_2 aerogels in high-performance insulation fields.

While ZrO_2–SiO_2 composite aerogels exhibit better thermal stability (up to 1000 °C) than the pure SiO_2 aerogels because zirconia exhibits high-temperature resistance, the unformed silica restrains the phase transition of zirconium [14]. They can be fabricated from zirconium precursor (mainly $ZrOCl_2$) and silicon precursor (mainly TEOS) by sol–gel process [15, 16]. To improve the strength and fragility of aerogels, two methods are usually used: (i) Functional polymers are added into aerogels and cross-link with them, such as polyurethane [17], epoxy [18], and polyethylene [19]. However, the addition of polymer weakens the aerogels' high-temperature resistance, due to the decomposition of polymer at high temperature. (ii) Inorganic fibers are introduced as the skeletons for the aerogels. Several inorganic fibers, such as glass fibers [20], quartz fibers [21], and sepiolite fibers [22] etc., have been used to fabricate fiber-reinforced aerogels.

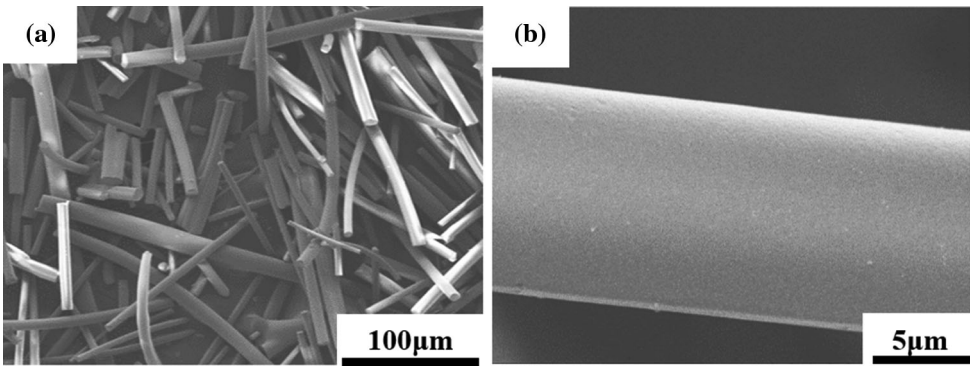

Fig. 1 SEM images of mullite fibers

However, these fibers tend to precipitate from the sols during the gelling process, which is fatal for the heat-insulating property. The agglomeration and deposition of fibers will result obviously in increasing thermal conductivity in the aerogels. To solve this problem, an effective way is to introduce gel coagulant to accelerate rapid gel.

Epoxide is a kind of proton scavengers to drive the hydrolysis and condensation of the hydrate metal species. It was widely used as gelation initiators in the fabrication of metal oxide aerogel monoliths [23–25]. Herein, mullite fibers-reinforced ZrO_2–SiO_2 (M/ZrO_2–SiO_2) aerogels are fabricated by introducing short-cut mullite fibers into ZrO_2–SiO_2 sols using epoxide as gelation accelerators. The addition of epoxides realizes rapid gelation of sol within 1 min, which avoids the agglomeration and deposition of mullite fibers in the ZrO_2–SiO_2 matrix. The microstructure of M/ZrO_2–SiO_2 aerogel composites is studied by SEM and TEM. The pore distributions of M/ZrO_2–SiO_2 aerogel composites are characterized by N_2 adsorption–desorption method. Meanwhile, the mechanical behavior and thermal conductivity with different mullite fiber factions are also studied. It is found that M/ZrO_2–SiO_2 aerogel composites with high strength and low thermal conductivity can be fabricated by this rapid gel method.

Experimental procedures

Raw materials

Commercially available polycrystalline mullite refractory fibers (99.5 %, Zhejiang Hongda Crystal Fiber Co., Ltd., China) were used as the reinforced skeleton for the M/ZrO_2–SiO_2 aerogels. Short-cut mullite fibers have the diameters in the range of 2–15 μm and the lengths in the range of 100–400 μm observed by SEM as shown in Fig. 1a, b. Zirconium oxychloride ($ZrOCl_2$, Tianjin Jiangtian Chemical Co., China) and tetraethylorthosilicate (TEOS, AR grade, Tianjin Jiangtian Chemical Co., China) were used as the zirconium and silicon precursors, respectively, and 1,2-epoxypropane (Po, AR grade, Tianjin Guangfu Chemical Co., China) was used as gelation promoter to ensure the rapid gelatin of sol. Nitric acid (HNO_3, AR grade, Tianjin Kemiou Chemical Co., China) was used as catalyst. Polyethylene glycol 600 (PEG, AR grade, Tianjin Guangfu Chemical Co., China) and formamide (FA, AR grade, Tianjin Guangfu Chemical Co., Chin) were, respectively, used as dispersant and dry control chemical agent.

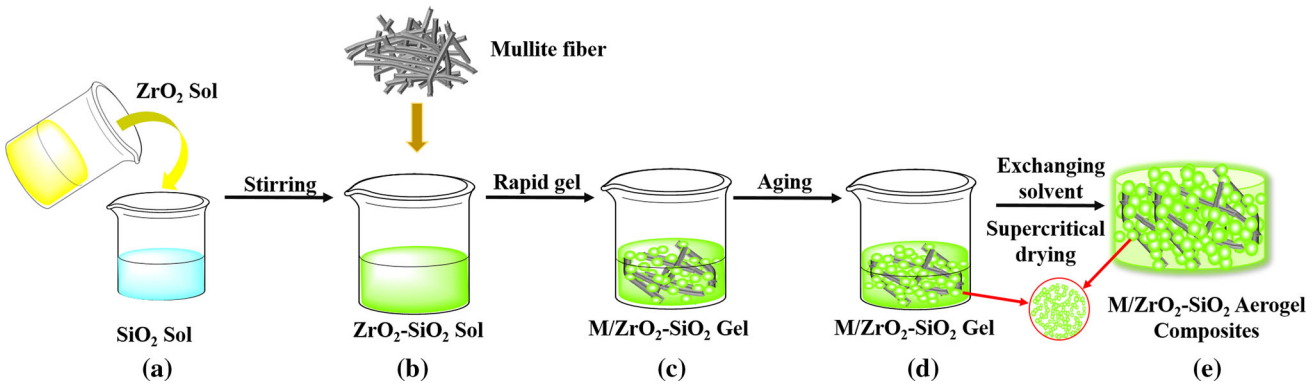

Fig. 2 Prepare processing of M/ZrO_2–SiO_2 aerogel composites

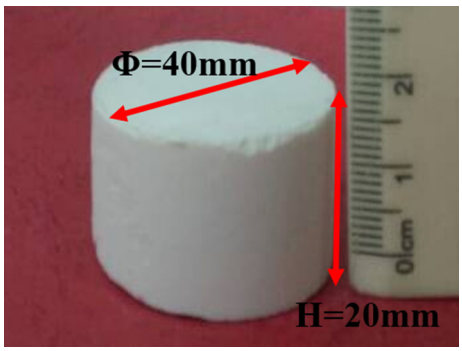

Fig. 3 Photograph of M/ZrO_2–SiO_2 aerogel composites with the diameter of 40 mm and the height of 20 mm

Experimental procedure

M/ZrO_2–SiO_2 aerogel composites are fabricated by introducing short-cut mullite fibers into ZrO_2–SiO_2 sol followed by a rapid gel method, as shown in Fig. 2. Firstly, TEOS was pre-hydrolyzed to ensure the homogenous reaction with $ZrOCl_2$ due to the slower hydrolysis rate of TEOS than that of $ZrOCl_2$ (Fig. 2a). The TEOS was dissolved in ethanol-aqueous solution under nitric acid to pre-hydrolyse for an hour. Afterwards, $ZrOCl_2$ was dissolved in ethanol-aqueous solution to get ZrO_2 sol. Then, the ZrO_2 sol was added into the acidifying SiO_2 sol to prepare the ZrO_2–SiO_2 sol under stirring. The mole ratio of $ZrOCl_2$:TEOS:HNO_3:H_2O:CH_3CH_2OH was 1:1:1.6:8:40. Secondly, short-cut mullite fibers were added into ZrO_2–SiO_2 sols to form homogenous mixture under magnetic stirring for 30 min (Fig. 2b), and then Po was added drop by drop to accelerate the transformation of the sol to gel within 1 min (Fig. 2c). Thirdly, the solution was transferred to Teflon molds and aged in 40 vol% TEOS ethanol solution for 3 days (30, 45, and 60 °C, respectively, for 1 day) in the oven (Fig. 2d). Finally, the excessive TEOS and water in the pores of gels were exchanged with ethanol for 4 times in 12 h, and then the gels were transferred into an autoclave for drying by high-temperature supercritical fluid drying method (Fig. 2e). The final critical temperature and pressure of the system were about 260 °C and 7.5 MPa, respectively. The supercritical state was kept for 0.5 h, and the autoclave was decompressed at a rate of 30 kPa/min. Finally, the M/ZrO_2–SiO_2 aerogel composites were obtained with mullite fibers as reinforcement phase in the ZrO_2–SiO_2 aerogels.

Characterization

The bulk densities (ρ) of the M/ZrO_2–SiO_2 aerogel composites were determined by measuring the volume (V) calculated by the dimensions of the samples and mass (M) of the monolithic sample ($\rho = M/V$). The porosity (P) was obtained from (P=) × 100 %, where V_a, V_b, V is the volume of aerogels, mullite fibers, and M/ZrO_2–SiO_2 composites, respectively. The nitrogen adsorption–desorption which had been isothermed at 77 K were characterized by a Micrometrics Quantachrome NOVA 2200e system after the sample was degassed in a vacuum at 150 °C for 240 min. The pore size distribution was calculated from the

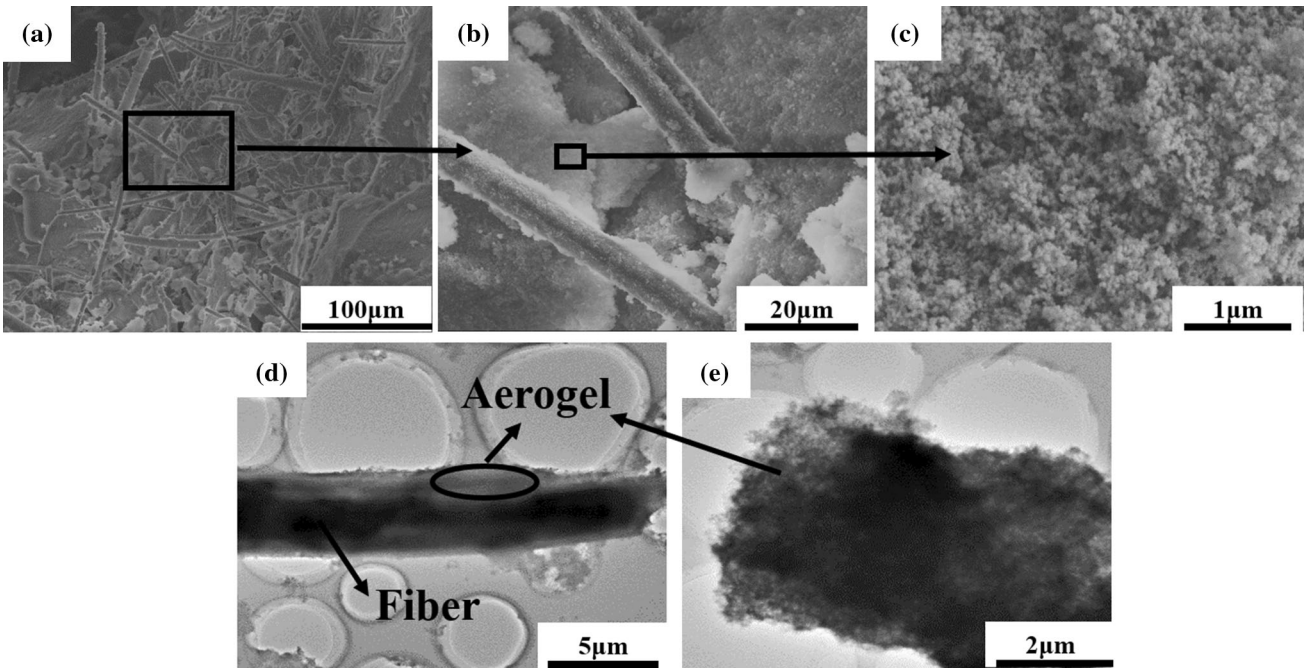

Fig. 4 SEM (**a**–**c**) and TEM (**d**, **e**) images of M/ZrO_2–SiO_2 aerogel composites

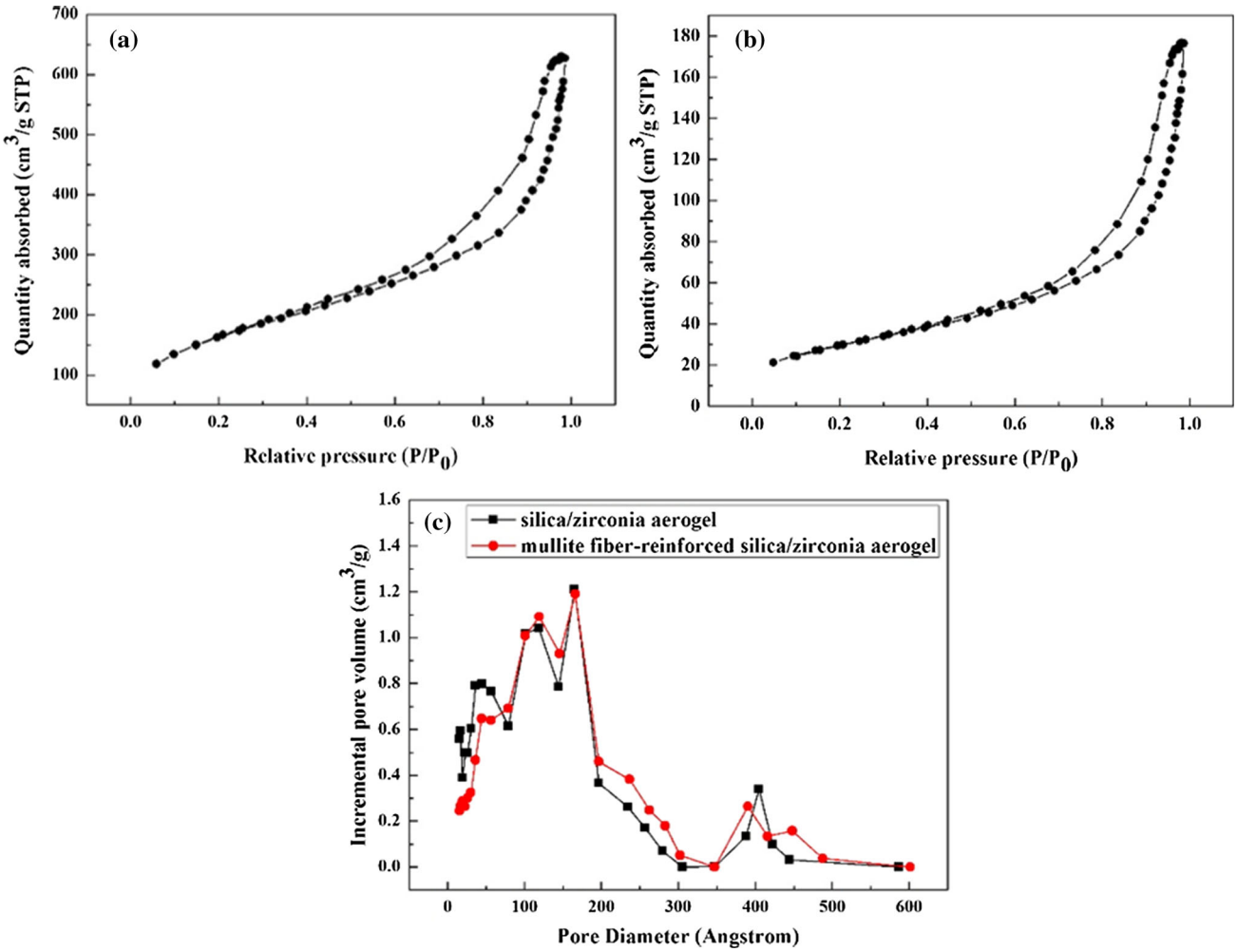

Fig. 5 N_2 adsorption–desorption isotherms of **a** ZrO_2–SiO_2 aerogel; **b** M/ZrO_2–SiO_2 aerogel composites containing 10 vol% mullite fibers; **c** their pore size distribution curves

data of the desorption branch of the isotherm using Barrett–Joyner–Halenda (BJH) method. The microstructures of the samples were characterized by scanning electron microscopy (SEM) with a TDCLS-4800 scanning electron microscope (Hitachi) and transmission electron microscopy (TEM) with a JEOL-200CX SEM. The thermal conductivity of the samples was measured at 25 °C using the transient hot-wire technique, in which a platinum hot-wire was squeezed between a pair of cylindrical aerogel blocks. The compressive strength was measured by a DL-15 digital mechanical strength tester with a loading speed of 0.05 mm/min in accordance with GB/T 1964-1996.

Results and discussion

M/ZrO_2–SiO_2 aerogel composites are fabricated from the mixture of short-cut mullite fibers and ZrO_2–SiO_2 sol with a rapid gel method. Figure 3 shows an integral M/ZrO_2–SiO_2 aerogel composites without crack, whose size is 40 mm in diameter and 20 mm in height. The densities of the ZrO_2–SiO_2 aerogel composites with different factions (from 0 to 10 %) of mullite fibers are in the range of 0.225–0.419 g cm^{-3} and corresponding porosities are in the range of 89–94 %.

Structure characterization

The microstructure of M/ZrO_2–SiO_2 aerogel composites has been analyzed by SEM and TEM compared with the pure ZrO_2–SiO_2 aerogels. SEM results shows that the M/ZrO_2–SiO_2 aerogel composites have a three-dimensional reticulated porous structure (Fig. 4c) similar to that of the pure ZrO_2–SiO_2 aerogels, which indicates the introduction of mullite fibers has no effect on the formation of aerogels. Mullite fibers are homogenously distributed in aerogels matrix, as showed in Fig. 4a, indicating rapid gelation is an effective method to solve the aggregation

Table 1 Physical, mechanical, and thermal properties of M/ZrO_2–SiO_2 aerogel composites with different volume fractions of mullite fibers

Fiber volume fraction (%)	Density (g cm^{-3})	Porosity (%)	Compressive strength (MPa)	Thermal conductivity (W m^{-1} K^{-1})
0	0.225	94	–	0.0268
4	0.274	93	0.286	0.0277
6	0.326	92	0.311	0.0270
8	0.382	90	0.369	0.0271
10	0.419	89	0.438	0.0273

problem of fibers. Image in high magnification (Fig. 4b) reveals that the mullite fibers combined well with the matrix. TEM also shows the mullite fiber are homogenously wrapped with the ZrO_2–SiO_2 phase without cracking or deboning (Fig. 4d), which may result from the excellent wettability between fibers and aerogel phase. Figure 4e shows the ZrO_2–SiO_2 phase possesses a three-dimensional reticulated porous structure, further indicating the formation of porous structure of aerogels.

N_2 adsorption–desorption isotherm curves of the pure ZrO_2–SiO_2 aerogels and the M/ZrO_2–SiO_2 aerogel composites with 10 vol% of fibers are showed in Fig. 5a, b. M/ZrO_2–SiO_2 aerogel composites show a typical type IV adsorption–desorption isotherm as the pure ZrO_2–SiO_2 aerogels, indicating the formation of mesoporous structures. The hysteresis loop for M/ZrO_2–SiO_2 aerogel composites corresponds to the H3 type, which is the characteristic of opened cylindrical pores [26, 27]. The pore size distribution curves of the two samples are showed in Fig. 5c. The curve of M/ZrO_2–SiO_2 aerogels is obtained by subtracting the mass of mullite fibers, because mullite fibers hardly make contribution to the pore diameter distribution in the mesoporous range. The pore sizes of both samples are in the range of 2–60 nm, further indicating that the mesoporous structure of the aerogels is not affected by the addition of mullite fibers, which are consistent with the SEM and TEM results (Fig. 4c, e). Therefore, M/ZrO_2–SiO_2 aerogel composites show a three-dimensional network of interconnected particles and continuously open mesoporous similarly with aerogels.

Property characterization

The mechanical properties of M/ZrO_2–SiO_2 aerogel composites with different volume fractions of mullite fibers are showed in Table 1. The compressive strength is defined as the stress at 10 % strain. The compressive strength of M/ZrO_2–SiO_2 aerogel composites rises from 0.286 to 0.438 MPa as the fraction of mullite fiber increased from 4 to 10 vol%. The stress–strain curves of M/ZrO_2–SiO_2 aerogel composites (Fig. 6) show three different stages under compression including two linear stages [Fig. 6 (1, 2)] and one densification stage [Fig. 6 (3)]. The composites with different contents of mullite fibers show the same linear trend in the first stage under the strain range of 0–2 %. The slopes of curves increase with the fibers fraction in the second linear stage. Lastly, the curves tend to be horizontal, revealing that the aerogels are compacted at the densification stage. The fracture behavior of M/ZrO_2–SiO_2 aerogel composites is quite different from the pure ZrO_2–SiO_2 aerogel due to the high strength of mullite fibers and the loading transfer of fibers in aerogels.

Pure ZrO_2–SiO_2 aerogel shows only a linear stage due to its brittle fracture property and usually breaks before 10 % compressive strain, as showed in Fig. 6a. Crack was induced by collapse of the pores (Fig. 7a) due to its low strength of nano porous structure when the aerogels were loaded. For M/ZrO_2–SiO_2 aerogel composites, the crack propagated similarly with that of the pure ZrO_2–SiO_2 aerogels in the first stage, while the load was transferred to fibers when crack tip touches with fibers as increasing the loading in the second stage. A great amount of bridged fibers are observed in the cracks as showed in Fig. 7b, c, which retard the crack propagation. Therefore, in M/ZrO_2–SiO_2 aerogel composites, stress field is formed around mullite fibers and the stress of crack tip is reduced because

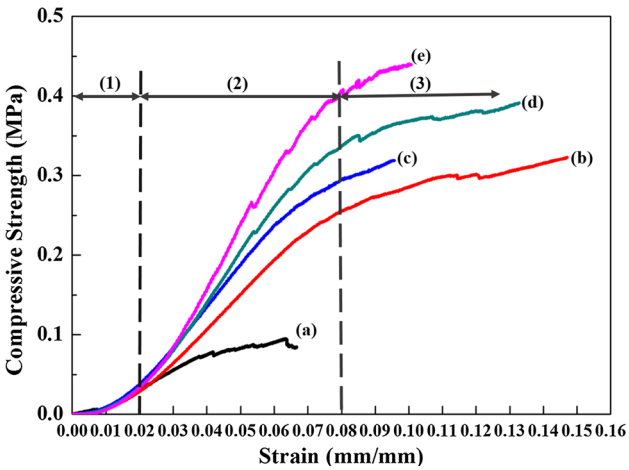

Fig. 6 Stress–strain curves of M/ZrO_2–SiO_2 aerogel composites with different volume fractions of mullite fibers: *a* 0 vol%; *b* 4 vol%; *c* 6 vol%; *d* 8 vol%; *e* 10 vol%.*1* first linear stage; *2* second linear stage; *3* densification stage

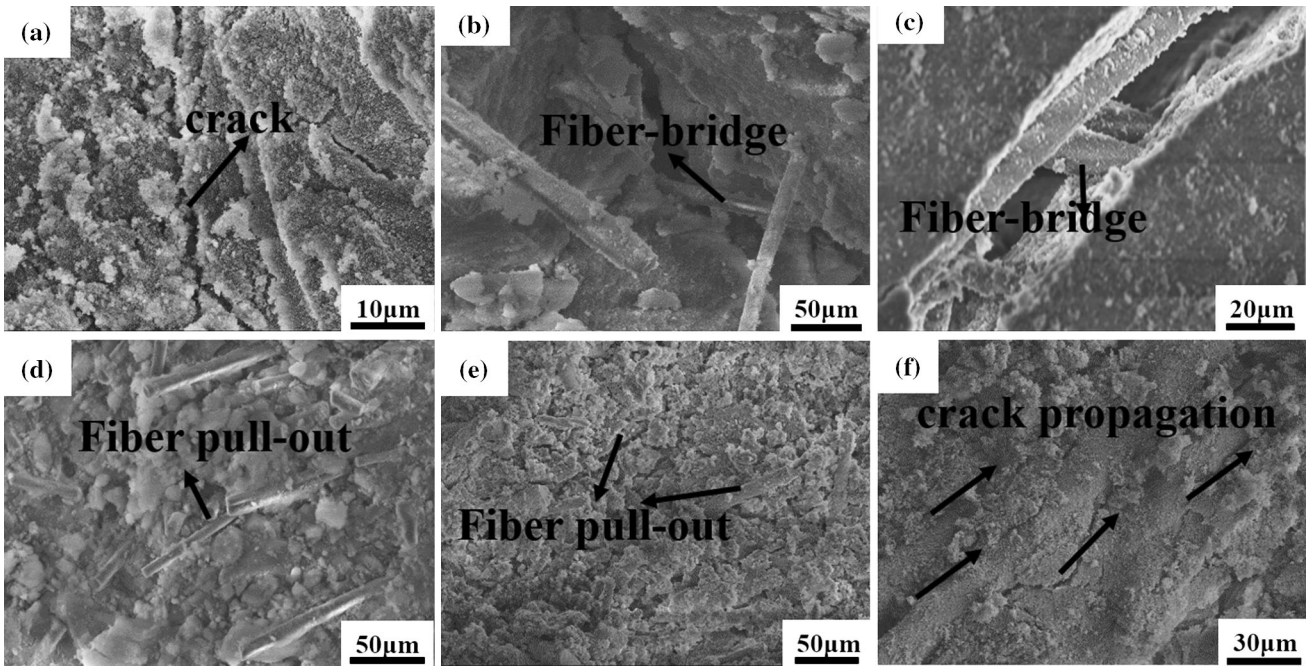

Fig. 7 SEM (**a**–**f**) images of M/ZrO_2–SiO_2 aerogel composites after compression resistance

mullite fibers slip off along the bonding interface of fibers and matrix under the extension stress (Fig. 7e, f). Meanwhile, an amount of energy is consumed to overcome the frictional work on the bonding interface of fibers and matrix when mullite fibers are pulled out from the matrix (Fig. 7d). The pull-out and fiber-bridge of fibers can improve the fragility of aerogels and the corresponding toughening mechanism of fibers in aerogels had been reported by Wang [28] and Li [29]. The mullite fibers can transfer the loading when the aerogels are compacted so that the strength and the tenacity are increased.

As showed in Table 1, the thermal conductivities of M/ZrO_2–SiO_2 aerogel composites don't increase with volume fraction of fibers. Moreover, the thermal conductivities of M/ZrO_2–SiO_2 aerogel composites are as low as that of the pure ZrO_2–SiO_2 aerogels. Jaesoek Ryu [30] reported that there are two patterns of the dispersion of fibers in aerogels matrix: (1) fibers overlapped each other and formed 'fiber–fiber' pattern, which helped produce heat-bridge so that the thermal conductivity would be increased; (2) fibers jointed with aerogels in the middle and formed 'fiber–aerogel–fiber' pattern. In the second pattern, the heat transfer could be separated by the aerogels with the pattern of fiber–aerogel–fiber and the heat-insulating property of composite aerogels would decrease. In our work, the 'fiber–aerogel–fiber' pattern exists in M/ZrO_2–SiO_2 aerogel composites instead of the 'fiber–fiber' pattern, as showed in Fig. 7(d), which is attributed to homogenous distribution of mullite fibers in the ZrO_2–SiO_2 matrix resulting from the rapid gelatin within 1 min by the addition of epoxides.

Conclusion

Mullite fiber-reinforced ZrO_2–SiO_2 composite aerogels have been prepared by introducing the short-cut mullite fiber into the ZrO_2–SiO_2 sol with a rapid gel method. The densities of M/ZrO_2–SiO_2 aerogel composites are in the range of 0.225–0.419 g/cm^3, and their porosities are of 89–94 %. They consist of three-dimensional reticulated porous structure similar with those of the pure ZrO_2–SiO_2 aerogels. The fibers homogeneously disperse into the matrix with good bonding. The toughening mechanism of fiber pull-out and fiber-bridge is also studied. M/ZrO_2–SiO_2 aerogel composites exhibit high compressive strength up to 0.438 MPa. Moreover, they have a thermal conductivity of 0.0270 W m^{-1} K^{-1}, which is as low as that of the pure ZrO_2–SiO_2 aerogels. Due to the simplicity of this rapid gel method, the M/ZrO_2–SiO_2 aerogel composites will be widely used in the thermal management application.

Acknowledgements We acknowledge the funding supports from National Natural Science Foundation of China (Grant No.: 51202157), Tianjin Research Program of Application Foundation and Advanced Technology (Grant No.: 14JCQNJC02800), and Independent Innovation Foundation of Tianjin University.

References

1. Feng J, Zhang C, Feng J (2011) Carbon aerogel composites prepared by ambient drying and using oxidized polyacrylonitrile fibers as reinforcements. ACS Appl Mater Interfaces 3(12):4796–4803
2. Wang X, Jana SC (2013) Synergistic Hybrid Organic-Inorganic Aerogels. ACS Appl Mater Interfaces 5(13):6423–6429
3. Hong SK, Yoon MY, Hwang HJ (2011) Fabrication of spherical silica aerogel granules from water glass by ambient pressure drying. J Am Ceram Soc 94(10):3198–3201
4. Zhao ZQ, Chen DR, Jiao XL (2007) Zirconia aerogels with high surface area derived from sols prepared by electrolyzing zirconium oxychloride solution: comparison of aerogels prepared by freeze-drying and supercritical CO_2 (l) extraction. J Phys Chem 111(50):18738–18743
5. Sachithanadam M, Joshi SC (2014) High strain recovery with improved mechanical properties of gelatin–silica aerogel composites post-binding treatment. J Mater Sci 49(1):163–179. doi:10.1007/s10853-013-7690-1
6. Hegde ND, Rao AV (2007) Physical properties of methyltrimethoxysilane based elastic silica aerogels prepared by the two-stage sol–gel process. J Mater Sci 42(16):6965–6971. doi:10.1007/s10853-006-1409-5
7. Maleki H, Durães L, Portugal A (2014) Synthesis of lightweight polymer-reinforced silica aerogels with improved mechanical and thermal insulation properties for space applications. Microporous Mesoporous Mater 197:116–129
8. Jung SM, Jung HY, Fang W (2014) A facile methodology for the production of in situ inorganic nanowire hydrogels/aerogels. Nano Lett 14(4):1810–1817
9. Schiffres SN, Kim KH, Hu L (2012) Gas diffusion, energy transport, and thermal accommodation in single-walled carbon nanotube aerogels. Adv Funct Mater 22(24):5251–5258
10. Bangi UKH, Dhere SL, Rao AV (2010) Influence of various processing parameters on water-glass-based atmospheric pressure dried aerogels for liquid marble purpose. J Mater Sci 45(11):2944–2951. doi:10.1007/s10853-010-4287-9
11. Koebel M, Rigacci A, Achard P (2012) Aerogel-based thermal superinsulation: an overview. J sol gel sci tech 63(3):315–339
12. Hayase G, Kugimiya K, Ogawa M (2014) The thermal conductivity of polymethylsilsesquioxane aerogels and xerogels with varied pore sizes for practical application as thermal superinsulators. J Mater Chem A 2(18):6525–6531
13. Nikel O, Anderson AM, Carroll MK (2011) Effect of uni-axial loading on the nanostructure of silica aerogels. J Non-cryst Solids 357(16):3176–3183
14. Xiong R, Li XL, He J (2014) Thermal stability of ZrO_2–SiO_2 aerogel modified by Fe(III) ion. J Sol-Gel Sci Tech 72(3):496–501
15. James BM, Edmond IK (1996) Acidic properties of silica-containing mixed oxide aerogels: preparation and characterization of zirconia-silica and comparison to titania-silica. J Catal 159(1):58–68
16. James BM, Edmond IK (1997) Control of mixed oxide textural and acidic properties by the sol-gel method. J Catal 35(3):269–292
17. Chang KJ, Wang YZ, Peng KC (2014) Preparation of silica aerogel/polyurethane composites for the application of thermal insulation. J Polym Res 21(1):1–9
18. Gupta N, Ricci W (2008) Processing and compressive properties of aerogel/epoxy composites. J Mater Process Tech 198(1):178–182
19. Silveira F, Brambilla R, da Silveira NP (2010) Effect of textural characteristics of Supported metallocenes on ethylene polymerization. J Mater Sci 45(7):1760–1768. doi:10.1007/s10853-009-4153-9
20. Kim CY, Lee JK, Kim BI (2008) Synthesis and pore analysis of aerogel–glass fiber composites by ambient drying method. Colloid Surf A 313:179–182
21. Buisson P, Pierre AC (2006) Immobilization in quartz fiber felt reinforced silica aerogel improves the activity of lipase in organic solvents. J Mol Catal B Enzym 39(1):77–82
22. Li XL, Wang QP, Li HL (2013) Effect of sepiolite fiber on the structure and properties of the sepiolite/silica aerogel composite. J Sol-Gel Sci Tech 67(3):646–653
23. Gash AE, Satcher JH, Simpson RL (2004) Monolithic nickel (II)-based aerogels using an organic epoxide: the importance of the counterion. J Non-crystal Solids 350:145–151
24. Baumann TF, Kucheyev SO, Gash AE (2005) Facile synthesis of a crystalline, high-surface-area sno2 aerogel. Adv Mater 17(12):1546–1548
25. Davis M, Hung-Low F, Hikal WM (2013) Enhanced photocatalytic performance of Fe-doped SnO2 nanoarchitectures under UV irradiation: synthesis and activity. J Mater Sci 48(18):6404–6409. doi:10.1007/s10853-013-7440-4
26. Kim CE, Yoon JS, Hwang HJ (2009) Synthesis of nanoporous silica aerogel by ambient pressure drying. J Sol-Gel Sci Tech 49(1):47–52
27. May M, Navarrete J, Asomoza M (2007) Tailored mesoporous alumina prepared from different aluminum alkoxide precursors. J Porous Mater 14(2):159–164
28. Wang J, Gloram PR (2001) Carbon cloth reinforced carbon aerogel films derived from resorcinol formaldehyde. J Porous Mater 8(2):159–165
29. Li L, Yalcin B, Nguyen BN (2009) Flexible nanofiber-reinforced aerogel (xerogel) synthesis, manufacture, and characterization. ACS Appl Mater Inter 1(11):2491–2501
30. Ryu J. Flexible aerogel superinsulation and its manufacture: U.S. Patent 6,068,882[P]. 2000-5-30